

University of Nebraska - Lincoln

DigitalCommons@University of Nebraska - Lincoln

Si-Hwang Liou Publications

Research Papers in Physics and Astronomy

June 1992

Crystalline orientations of $\text{Ti}_2\text{Ba}_2\text{Ca}_2\text{Cu}_3\text{O}_x$ grains on MgO, SrTiO_3 , and LaAlO_3 substrates

Sy_Hwang Liou

University of Nebraska-Lincoln, sliou@unl.edu

C.Y. Wu

University of Nebraska - Lincoln

Follow this and additional works at: <https://digitalcommons.unl.edu/physicsliou>



Part of the [Physics Commons](#)

Liou, Sy_Hwang and Wu, C.Y. , "Crystalline orientations of $\text{Ti}_2\text{Ba}_2\text{Ca}_2\text{Cu}_3\text{O}_x$ grains on MgO, SrTiO_3 , and LaAlO_3 substrates" (1992). *Si-Hwang Liou Publications*. 38.

<https://digitalcommons.unl.edu/physicsliou/38>

This Article is brought to you for free and open access by the Research Papers in Physics and Astronomy at DigitalCommons@University of Nebraska - Lincoln. It has been accepted for inclusion in Si-Hwang Liou Publications by an authorized administrator of DigitalCommons@University of Nebraska - Lincoln.

Crystalline orientations of $\text{Ti}_2\text{Ba}_2\text{Ca}_2\text{Cu}_3\text{O}_x$ grains on MgO , SrTiO_3 , and LaAlO_3 substrates

S. H. Liou and C. Y. Wu

Behlen Laboratory of Physics and Center for Materials Research and Analysis, University of Nebraska-Lincoln, Lincoln, Nebraska 68588-0111

(Received 14 February 1992; accepted for publication 17 March 1992)

Crystalline orientations of $\text{Ti}_2\text{Ba}_2\text{Ca}_2\text{Cu}_3\text{O}_x$ grains in magnetron sputtered films on MgO (001), SrTiO_3 (001), and LaAlO_3 (001) substrates were investigated by scanning electron microscopy. In contrast to the nearly single crystalline films on the lattice matched substrates SrTiO_3 and LaAlO_3 , films on the MgO (001) substrate, being polycrystalline in nature, exhibit several preferred in-plane grain orientations. These orientations agree well with a simplified theory of near-coincidence site lattices between $\text{Ti}_2\text{Ba}_2\text{Ca}_2\text{Cu}_3\text{O}_x$ and MgO .

Single crystalline MgO , SrTiO_3 , and LaAlO_3 substrates are popular for the deposition of high T_c superconducting oxide thin films. The growth behavior of superconducting phases on these substrates is very different. The microstructure of $\text{YBa}_2\text{Cu}_3\text{O}_{7-\delta}$ films on MgO , SrTiO_3 , and LaAlO_3 substrates has been studied intensively by several groups.¹⁻⁴ The films of $\text{YBa}_2\text{Cu}_3\text{O}_{7-\delta}$ grown on the lattice matched SrTiO_3 (001) and LaAlO_3 (001) substrates are usually epitaxial and the grains are oriented in three dimensions. However, the films on the lattice mismatched MgO (001) substrate are generally polycrystalline, but it has been observed that the grains may align to certain directions with respect to the MgO axes.⁵

In this letter, we report the results of the growth of $\text{Ti}_2\text{Ba}_2\text{Ca}_2\text{Cu}_3\text{O}_x$ superconducting phase on the (001) surfaces of MgO , SrTiO_3 , and LaAlO_3 substrates. We have observed that the growth behavior of Tl-based superconductors on these substrates is similar to that of $\text{YBa}_2\text{Cu}_3\text{O}_{7-\delta}$.

Thin films of $\text{Ti}_2\text{Ba}_2\text{Ca}_2\text{Cu}_3\text{O}_x$ were prepared on MgO (001), SrTiO_3 (001), and LaAlO_3 (001) substrates by magnetron sputtering from a stoichiometric target. The detail of thin-film deposition has been reported elsewhere.⁶ The film thickness was controlled based on the known deposition rate to about 5000 Å. The annealing was done in a sealed ceramic tube where the film was wrapped in gold foil with a compressed Tl compound to maintain the thallium vapor pressure. The annealing temperatures were 880°–890 °C, which were about 10 °C higher than normally used to promote granular growths.

The film structure was confirmed as $\text{Ti}_2\text{Ba}_2\text{Ca}_2\text{Cu}_3\text{O}_x$ phase by x-ray diffraction. An x-ray θ - 2θ scan of a film grown on (001) MgO substrate is shown in Fig. 1. As seen in this figure, all the major diffraction peaks can be assigned to (00 l) of the $\text{Ti}_2\text{Ba}_2\text{Ca}_2\text{Cu}_3\text{O}_x$ phase, indicating that the film is highly oriented with c -axis perpendicular to the film-substrate interface plane. This alignment may be simply due to the fact that the c axis is the slow growing direction and the a , b axes are the fast growing directions as evident in $\text{YBa}_2\text{Cu}_3\text{O}_{7-\delta}$, Bi-Sr-Ca-Cu-O , and Tl-Ba-Ca-Cu-O systems. The film composition was studied by energy dispersive x-ray spectroscopy (EDAX). Table I lists the compositions at several areas of a Tl film on LaAlO_3 substrate. These areas are labeled in the scanning

electron micrograph shown in Fig. 2(a). The film is populated with square platelike grains. Their compositions are close to the stoichiometry, as are those of the bar-shaped grains. These bar-shaped grains could be oriented with c -axis parallel to the interface plane although it is predominant with its c -axis perpendicular. In addition, the film also displays some irregular plates with barium rich composition. The small dots on the top of the plates are very rich in calcium. They seem to be excess materials to the preferred stoichiometry and exiled to the surface.

The morphology was studied by scanning electron microscopy (SEM). The SEM graphs of films on three different substrates are shown in Figs. 2 and 3. These films display many large rectangular plates with (001) surface, i.e., their c -axes are normal to the substrate surface.

For the films on SrTiO_3 (001) and LaAlO_3 (001) substrates, the epitaxial growth is evident^{7,8} as previously reported. This is typified in the square platelike films on LaAlO_3 (001) and SrTiO_3 (001) shown in Fig. 2. As can be seen in these SEM graphs, the edges of almost all the plates, presumably being [110] direction (or its equivalent) of the crystal, run approximately along 45° with respect to the edges of the graphs, which were known to be the [100] or [010] axis of the substrates. The epitaxial growth is

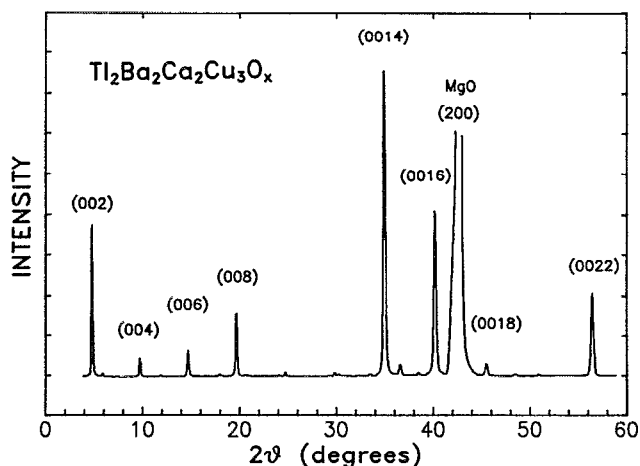


FIG. 1. X-ray diffraction pattern (Cu radiation) of a $\text{Ti}_2\text{Ba}_2\text{Ca}_2\text{Cu}_3\text{O}_x$ film on MgO (001) substrate showing $\text{Ti}_2\text{Ba}_2\text{Ca}_2\text{Cu}_3\text{O}_x$ phase with c -axis normal to the surface.

TABLE I. The film composition at various regions labeled in Fig. 2(a).

	Composition			
	Tl	Ba	Ca	Cu
A. Square plate	1.3	2.0	2.1	3.4
B. Dot	2.0	0.2	7.4	2.0
C. Irr. plate	1.9	3.2	2.0	3.2
D. Dot	2.0	0.4	3.5	0.8
E. Bar	1.4	2.0	2.0	2.8

expected because of the close match of lattice constants between the deposited Tl film and the substrates. Having established the fact that the c -axis of $\text{Tl}_2\text{Ba}_2\text{Ca}_2\text{Cu}_3\text{O}_x$ is perpendicular to the substrate (001) surface, we can treat the in-plane structure of the tetragonal $\text{Tl}_2\text{Ba}_2\text{Ca}_2\text{Cu}_3\text{O}_x$ as a square lattice and consider only two-dimensional matches. The lattice constant of $\text{Tl}_2\text{Ba}_2\text{Ca}_2\text{Cu}_3\text{O}_x$ ($a=3.82$ Å) is very close to those of the substrates ($a=3.91$ Å for SrTiO_3 and $a=3.788$ Å for LaAlO_3). In both cases, the

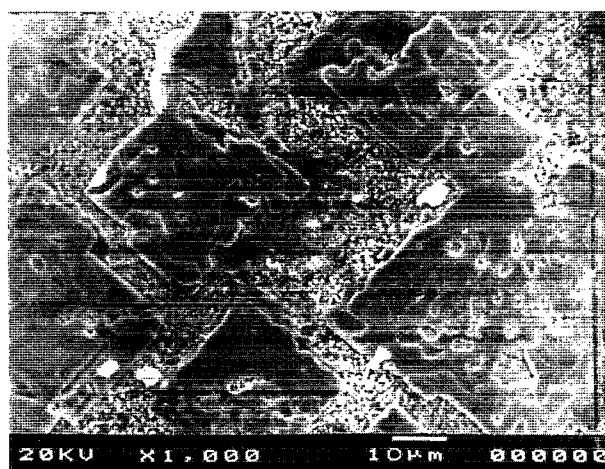
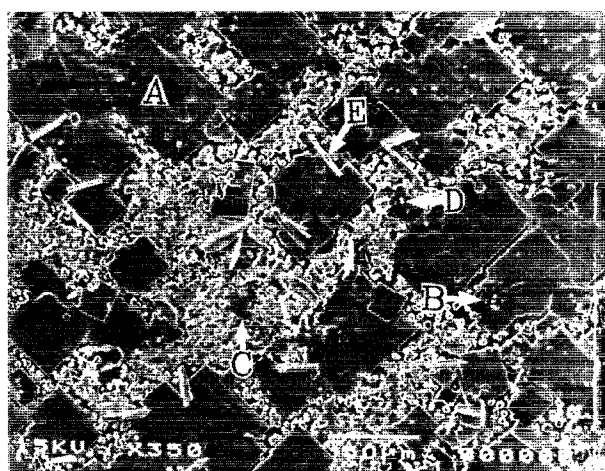


FIG. 2. Scanning electron micrographs showing epitaxial growth of $\text{Tl}_2\text{Ba}_2\text{Ca}_2\text{Cu}_3\text{O}_x$ films on (a) LaAlO_3 (001) and (b) SrTiO_3 (001). The compositions at the indicated areas in (a) are listed in Table I. The vertical direction of the graphs coincides with the [100] direction of the substrates.

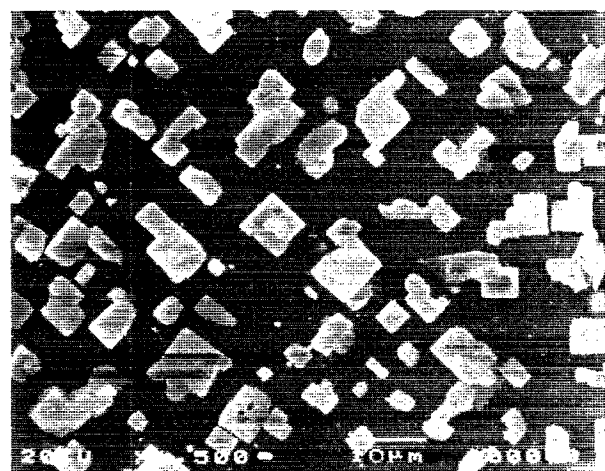
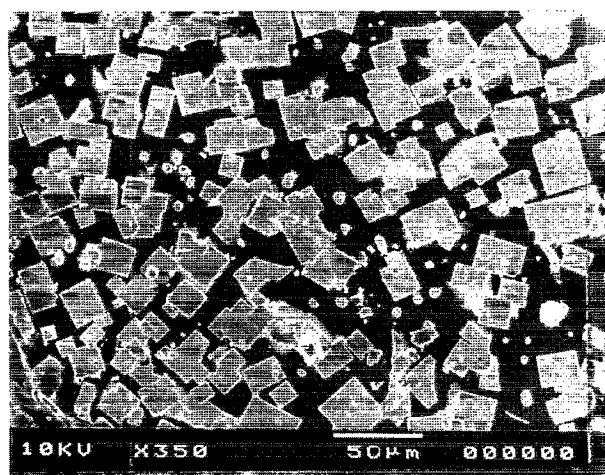


FIG. 3. Scanning electron micrographs of a $\text{Tl}_2\text{Ba}_2\text{Ca}_2\text{Cu}_3\text{O}_x$ film on MgO (001). (a) Shows the polycrystalline growth behavior, and (b) shows the popular growth directions. The vertical direction of the graphs coincides with the [100] direction of the substrate.

lattice misfits are very small (2% for SrTiO_3 substrate and less than 1% for LaAlO_3 substrate).

The situation is different with the MgO substrate. The lattice constant of MgO is 4.22 Å, with lattice misfit almost 10% between the Tl film and substrate MgO (001) on the basal plane. The Tl film is thus generally polycrystalline. This can be seen in Fig. 3(a). Unlike those well-oriented grains on LaAlO_3 and SrTiO_3 substrates shown in Fig. 2, the isolated square grains here do not show a similar in-plane alignment. These square grains being isolated may be a manifestation of island growth behavior as suggested for $\text{YBa}_2\text{Cu}_3\text{O}_{7-\delta}$.⁹ Careful examination on the grain orientation reveals that these grains have a tendency to align to certain distinct directions. We measured the misorientation angles θ , that is the relative orientation of the two lattices, in particular, it is the angles between [001] of $\text{Tl}_2\text{Ba}_2\text{Ca}_2\text{Cu}_3\text{O}_x$ and [100] of MgO , and entered them into a histogram. Here the edges of the rectangular grains were assumed to be [110] direction (or its equivalent) of $\text{Tl}_2\text{Ba}_2\text{Ca}_2\text{Cu}_3\text{O}_x$ crystals, similar to those on LaAlO_3 or SrTiO_3 substrate. The misorientation angles are reduced to

TABLE II. Configurations of "near-coincidence" site lattices between $\text{Ti}_2\text{Ba}_2\text{Ca}_2\text{Cu}_3\text{O}_x$ and MgO , with $\sigma_{\text{MgO}} < 25$ and $\delta < 3\%$, except for the cases with $\theta = 0^\circ$ and $\theta = 18.4^\circ$.

k	MgO		TBCCO			Misfit	Misorientation	
	l	σ	m	n	σ	δ	θ	
1	0	1	1	0	1	9.90%	0.0°	
2	0	4	2	1	5	1.25%	26.6°	
3	0	9	3	1	10	4.64%	18.4°	
3	2	13	4	0	16	0.48%	33.7°	
4	1	17	4	2	20	1.78%	40.6° ^a	12.5°
4	2	20	4	3	25	1.25%	26.6°	10.3°
4	3	25	4	4	32	2.44%	8.1°	15.1°
4	3	25	5	2	29	2.48%	31.3°	
5	0	25	4	4	32	2.44%	45.0°	
5	0	25	5	2	29	2.48%	21.8°	

^aNot observed so far.

$0^\circ < \theta < 45^\circ$ because of the fourfold rotational and mirror symmetries of both the tetragonal $\text{Ti}_2\text{Ba}_2\text{Ca}_2\text{Cu}_3\text{O}_x$ and the substrate MgO . We observed several preferred orientations where the misorientation angles peaked in the histogram. We also found that these preferred angles can closely match those calculated using the coincidence site lattice theory as indicated in Table II.

The coincidence site lattice theory¹⁰ has been used to explain the $\text{YBa}_2\text{Cu}_3\text{O}_{7-\delta}$ grain growth on MgO .⁵ The theory involves two interpenetrating lattices, in our case, due to the *c*-axis alignment, two interfacing two-dimensional square lattices. There may exist some special misorientation for which an infinite number of lattice points coincide with each other between the two lattices. These coincidence lattice points (or coincidence sites) form a lattice called the coincidence site lattice. The in-plane coincidence site lattice cells can be characterized by the parameter σ , which is the ratio of the matching cell area to the area occupied by each crystal lattice site on the interfacing plane.

The lattice constants of $\text{Ti}_2\text{Ba}_2\text{Ca}_2\text{Cu}_3\text{O}_x$ and MgO are incommensurate, therefore there would be no exact coincidence between these two lattices. We use the so called "near-coincidence" model, in which the lattice points of the two lattices can nearly match.

Let *a* be the lattice constant of the square lattice MgO with unit vectors ($\mathbf{a}_1, \mathbf{a}_2$). The translation vector can be written as $T_a = k\mathbf{a}_1 + l\mathbf{a}_2$, thus the length is given by $a\sqrt{\sigma_a}$ where $\sigma_a = k^2 + l^2$. Similar definitions for the square lattice $\text{Ti}_2\text{Ba}_2\text{Ca}_2\text{Cu}_3\text{O}_x$ are the lattice constant *b*, unit vectors ($\mathbf{b}_1, \mathbf{b}_2$), translation vector $T_b = m\mathbf{b}_1 + n\mathbf{b}_2$, and $\sigma_b = m^2 + n^2$. The degree of the mismatch between the two lattices is measured by misfit $\delta = 2(a\sqrt{\sigma_a} - b\sqrt{\sigma_b}) / (a\sqrt{\sigma_a} + b\sqrt{\sigma_b})$.

The low interfacial energy configurations can be characterized by small lattice misfit δ and high density of "near-coincidence" sites (i.e., small σ). Table II lists all the possible configurations from near-coincidence site lattice theory with $\sigma_{\text{MgO}} < 25$ and $\delta < 3\%$, except for $\theta = 0^\circ$ with $\delta = 9.9\%$ and $\theta = 18.4^\circ$ with $\delta = 4.6\%$. All the listed misorientations have been observed within an uncertainty of 1° , except for the case with $\theta = 40.6^\circ$, which has not been observed so far.

As can be seen in Table II, those preferred orientations correspond to relatively high density of coincidence sites and generally low misfit, although in some cases the misfit is high, for example, the misfit for 0° misorientation, i.e., the square on square case, is as high as 9.9%. According to the van der Merwe theory,¹¹ the stress caused by the lattice misfit can be released if the interaction between the atoms in the film is stronger than that between the adatoms and the substrate. In this case, the first layer atoms of the film may not be at the lowest energy position. In fact, the Ti film can be grown on MgO with populated 0° misorientation as shown in Fig. 3(b). Our studies show that 0° and 45° misorientations are most likely to be observed. There seems no correlation between the degree of misfit and the population of growth orientations.

In summary, $\text{Ti}_2\text{Ba}_2\text{Ca}_2\text{Cu}_3\text{O}_x$ grains are epitaxially grown on SrTiO_3 (001) and LaAlO_3 (001) while on MgO (001) they are locked into a few directions prescribed by a simplified theory of near-coincidence site lattice. The growth behavior is similar to that of the $\text{YBa}_2\text{Cu}_3\text{O}_{7-\delta}$ superconductor.

This work was supported by the Nebraska Energy Office and NASA Lewis Grant NAG 3-886.

¹S. T. Lee, S. Chen, L. S. Hung, and G. Braunstein, Appl. Phys. Lett. **55**, 286 (1989).

²M. G. Norton, L. A. Tietz, S. R. Summerfelt, and C. B. Carter, Appl. Phys. Lett. **55**, 2348 (1989).

³R. Ramesh, D. M. Hwang, T. S. Ravi, A. Inam, J. B. Barner, L. Nazar, S. W. Chan, C. Y. Chen, B. Dutta, T. Venkatesan, and X. D. Wu, Appl. Phys. Lett. **56**, 2243 (1990).

⁴J. A. Kittl, C. W. Nieh, D. S. Lee, and W. L. Johnson, Appl. Phys. Lett. **56**, 2468 (1990).

⁵D. M. Hwang, T. S. Ravi, R. Ramesh, S.-W. Chan, C. Y. Chen, L. Nazar, X. D. Wu, A. Inam, and T. Venkatesan, Appl. Phys. Lett. **57**, 1690 (1990).

⁶S. H. Liou, Mater. Res. Soc. Symp. Proc. **169**, 667 (1990).

⁷D. J. Werder and S. H. Liou, Physica C **179**, 430 (1991).

⁸C. H. Chen, M. Hong, D. J. Werder, J. Kwo, S. H. Liou, and D. D. Bacon, Appl. Phys. Lett. **54**, 1579 (1989).

⁹H. U. Krebs, Ch. Krauns, X. Yang and U. Geyer, Appl. Phys. Lett. **59**, 2180 (1991).

¹⁰R. W. Balluffi, A. Brokman, and A. H. King, Acta Metall. **30**, 1453 (1982).

¹¹F. C. Frank and J. H. van der Merwe, Proc. R. Soc. London A **198**, 205 (1949).